International Journal of Signal Processing, Image Processing and Pattern Recognition
Vol.9, No.12, (2016), pp.135-152
http://dx.doi.org/10.14257/ijsip.2016.9.12.14

Frequency Spectrum Customization and Optimization by Using Monte Carlo Method for Random Space Vector Pulse Width Modulation Strategy

Guoqiang Chen and Jianli Kang

School of Mechanical and Power Engineering, Henan Polytechnic University, Jiaozuo, 454000, China
jz97cgq@163.com

Abstract

The spectrum of the random space vector pulse width modulation (SVPWM) strategy is extremely complicated due to the random variable. A new algorithm based on the Monte Carlo method is proposed to optimize and customize the frequency spectrum of the random SVPWM strategy. A universal theoretical spectrum computation method is given for the SVPWM strategy firstly. In addition, the key procedure of the proposed algorithm is presented. Finally, several computation examples are provided to verify the effectiveness and feasibility. The analysis and computation examples show that the proposed algorithm has several advantages, and the results verify its convenience and feasibility.

Keywords: *Space vector pulse width modulation, Monte Carlo, Maximum harmonic amplitude, Random variable*

1. Introduction

In the motor controlling application, the undesirable harmonic inevitably results from the space vector pulse width modulation (SVPWM) strategy [1-2], which causes many problems, such as dynamic characteristic of the motor system, loss, electromagnetic compatibility and audible noise [3-11]. The deterministic SVPWM strategy presents cluster harmonics with very large amplitudes around the integer multiple switching frequencies, which makes the case more serious. Therefore, the random SVPWM strategy has been proposed and studied to suppress the harmonics with large amplitudes [4-12]. However, the spectrum of the random SVPWM strategy is extremely complicated due to the random variable, so it is difficult to accurately predict the maximum harmonic amplitude that is a key index to assess the performance of a modulation strategy. An efficient and effective algorithm is therefore needed of which the maximum harmonic amplitude and even the harmonic spectrum can be customized with high accuracy [13]. In this paper, a new algorithm based on the Monte Carlo method is proposed to customize and optimize the frequency spectrum of the random SVPWM strategy. Furthermore the maximum amplitude can be customized. The key steps of the algorithm are presented. Finally, the proposed algorithm is verified through several examples.

2. Random SVPWM Strategy

The 8 basic space vectors are shown in Figure 1(a), that are corresponding to the 8 permissible states of the classic two-level inverter. For an arbitrary reference/command voltage vector, for example $\vec{U}_s$ residing in the first sextant, the on-state duration time T_1, T_2 and T_0 of the three basic vectors are determined by the

ISSN: 2005-4254 IJSIP

identical volt-second balance at the periodical time interval/switching period T_s using Equation (1). The commonly used 7-segment pattern SVPWM strategy is shown in Figure 1(b).

$$T_s\vec{U}_s = T_1\vec{U}_1 + T_2\vec{U}_2 \tag{1}$$

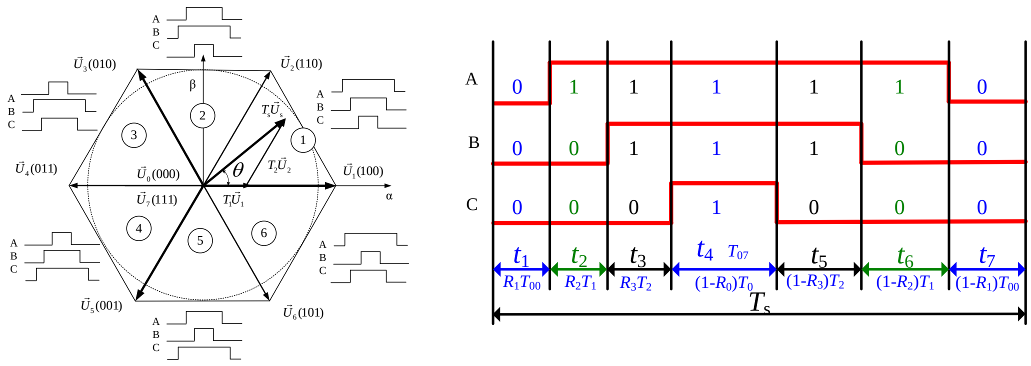

(a) Basic Space Vectors (b) 7-segment SVPWM Pattern in the First Sextant

Figure 1. Vector Diagram and Vector Summation Method

Usually the switching pulse signals in Figure 1 (b), is symmetrical in the deterministic SVPWM strategy. That is to say, $t_1 = t_7$, $t_2 = t_6$, $t_3 = t_5$, and $t_1 + t_7 = t_4$. However, the ratio of $(t_1 + t_7)$ to t_4 is controlled by a random variable R_0, the ratio of t_1 to t_7 is controlled by a random variable R_1, the ratio of t_2 to t_6 is controlled by a random variable R_2, and the ratio of t_3 to t_5 is controlled by a random variable R_3 in the random SVPWM strategy. The above relationship can be expressed as

$$\begin{cases} T_0 = T_s - (T_1 + T_2) \\ T_{00} = R_0 T_0 \qquad\qquad (0 \le R_0 \le 1) \\ T_{07} = (1 - R_0) T_0 \end{cases} \tag{2}$$

where the duration time T_{00} and T_{07} are for $\vec{U}_0$ and $\vec{U}_7$, respectively.

$$\begin{cases} t_1 = R_1 T_{00} \\ t_2 = R_2 T_1 \\ t_3 = R_3 T_2 \\ t_4 = T_{07} \\ t_5 = (1 - R_3) T_2 \\ t_6 = (1 - R_2) T_1 \\ t_7 = (1 - R_1) T_{00} \end{cases} \qquad \begin{pmatrix} 0 \le R_1 \le 1 \\ 0 \le R_2 \le 1 \\ 0 \le R_3 \le 1 \end{pmatrix} \tag{3}$$

3. Harmonic Frequency Spectrum Computation of SVPWM Strategy

Any periodic signal $x(t)$ with the period T_0 can be decomposed into the sum of a (possibly infinite) set of simple oscillating functions, namely sines and cosines (or, equivalently, complex exponentials), and therefore

$$x(t) = \frac{a_0}{2} + \sum_{k=1}^{\infty}\left[a_k \cos k\omega_0 t + b_k \sin k\omega_0 t\right] = \frac{a_0}{2} + \sum_{k=1}^{\infty} A_k \sin\left(k\omega_0 t + \varphi_k\right) \tag{4}$$

where $\omega_0 = 2\pi/T_0$, and the Fourier coefficients are given by

$$\begin{cases} a_0 = \dfrac{1}{T_0}\int_{-\frac{T_0}{2}}^{\frac{T_0}{2}} x(t)\mathrm{d}t \\ a_k = \dfrac{2}{T_0}\int_{-\frac{T_0}{2}}^{\frac{T_0}{2}} x(t)\cos\left(k\omega_0 t\right)\mathrm{d}t \\ b_k = \dfrac{2}{T_0}\int_{-\frac{T_0}{2}}^{\frac{T_0}{2}} x(t)\sin\left(k\omega_0 t\right)\mathrm{d}t \\ A_k = \sqrt{a_k^2 + b_k^2} \\ \varphi_k = \arctan\dfrac{a_k}{b_k} \end{cases} \tag{5}$$

Equation (4) can also be expressed as

$$x(t) = \sum_{k=-\infty}^{\infty} c_k \mathrm{e}^{\mathrm{j}k\omega_0 t} \tag{6}$$

where

$$c_k = \begin{cases} \left(a_k - \mathrm{j}b_k\right)/2 & k > 0 \\ a_0 & k = 0 \\ \left(a_k + \mathrm{j}b_k\right)/2 & k < 0 \end{cases} \tag{7}$$

The coefficients c_k can also been given by

$$c_k = \frac{1}{T_0}\int_{-\frac{T_0}{2}}^{\frac{T_0}{2}} x(t)\mathrm{e}^{-\mathrm{j}k\omega_0 t}\mathrm{d}t \tag{8}$$

The three-phase switching signals that control the power switches in the upper arms of the inverter, for example the IGBTs (Insulated Gate Bipolar Transistors), are periodic, which are shown in Figure 1. Figure 2, shows the switching signal of one phase (that is Phase A, B or C) in a period T_0 and in a switching period T_s. If there are N switching periods T_s in a period T_0 , the switching signal $x(t)$ shown in Figure 2, can be decomposed into the sum of N square wave signals.

$$x(t) = \sum_{i=1}^{N} x_i(t) \tag{9}$$

The i-th square wave signal $x_i(t)$ in a period T_0 is given by

$$x_i(t) = \begin{cases} 0 & t < \left(i-1\right)T_\mathrm{s} + T_\mathrm{b} \text{ or } t < iT_\mathrm{s} - T_\mathrm{e} \\ 1 & \left(i-1\right)T_\mathrm{s} + T_\mathrm{b} \le t \le iT_\mathrm{s} - T_\mathrm{e} \end{cases} \tag{10}$$

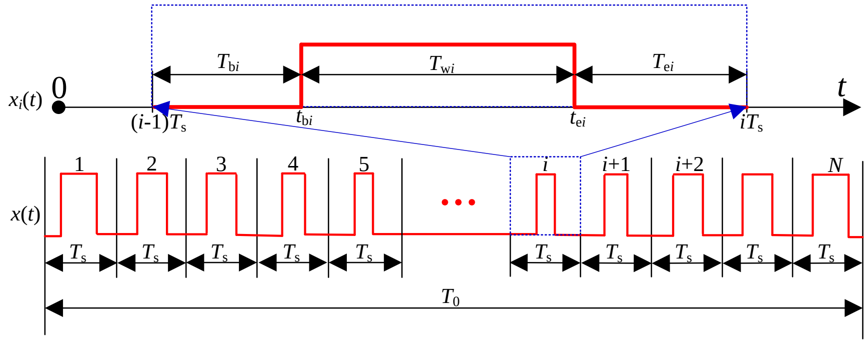

Figure 2. Periodic Rectangular Pulse Signal in the Fundamental and Switching Periods

According to Equation (8), the coefficients $c_{ki}(k=1,2,3,\cdots)$ for $x_i(t)$ can be expressed as

$$\begin{aligned} c_{ki} &= \frac{1}{T_0}\int_{-\frac{T_0}{2}}^{\frac{T_0}{2}} x_i(t)\mathrm{e}^{\text{-j}k\omega_0 t}\mathrm{d}t = \frac{1}{T_0}\int_{t_{bi}}^{t_{ei}} x_i(t)\mathrm{e}^{\text{-j}k\omega_0 t}\mathrm{d}t \\ &= \frac{1}{T_0}\frac{1}{\text{-j}k\omega_0}\mathrm{e}^{\text{-j}k\omega_0 t}\Big|_{t_{bi}}^{t_{ei}} = \frac{\mathrm{j}}{kT_0\omega_0}\left(\mathrm{e}^{\text{-j}k\omega_0 t_{ei}} - \mathrm{e}^{\text{-j}k\omega_0 t_{bi}}\right) \end{aligned} \tag{11}$$

Therefore the harmonic coefficients c_k for $x(t)$ can be expressed as

$$c_k = \sum_{i=1}^{N} c_{ki} = \frac{\mathrm{j}}{kT_0\omega_0}\sum_{i=1}^{N}\left(\mathrm{e}^{\text{-j}k\omega_0 t_{ei}} - \mathrm{e}^{\text{-j}k\omega_0 t_{bi}}\right) \tag{12}$$

So the amplitude for the k-th $(k=1,2,3,\cdots)$ harmonic can be computed as

$$A_k = 2|c_k| = 2\left|\frac{\mathrm{j}}{kT_0\omega_0}\sum_{i=1}^{N}\left(\mathrm{e}^{\text{-j}k\omega_0 t_{ei}} - \mathrm{e}^{\text{-j}k\omega_0 t_{bi}}\right)\right| \tag{13}$$

4. Harmonic Spectrum Customization and Optimization Algorithm

Based on the accurate theoretical harmonic spectrum (that can be expediently given by Equation (12)), the harmonic amplitudes and the maximum amplitude can be computed using Equation (13). A harmonic amplitude customization and optimization algorithm (using the Monte Carlo method) is proposed to aid in selecting the random numbers shown Equations (2) and (3). The algorithm is shown in Figure 3 and as follows.

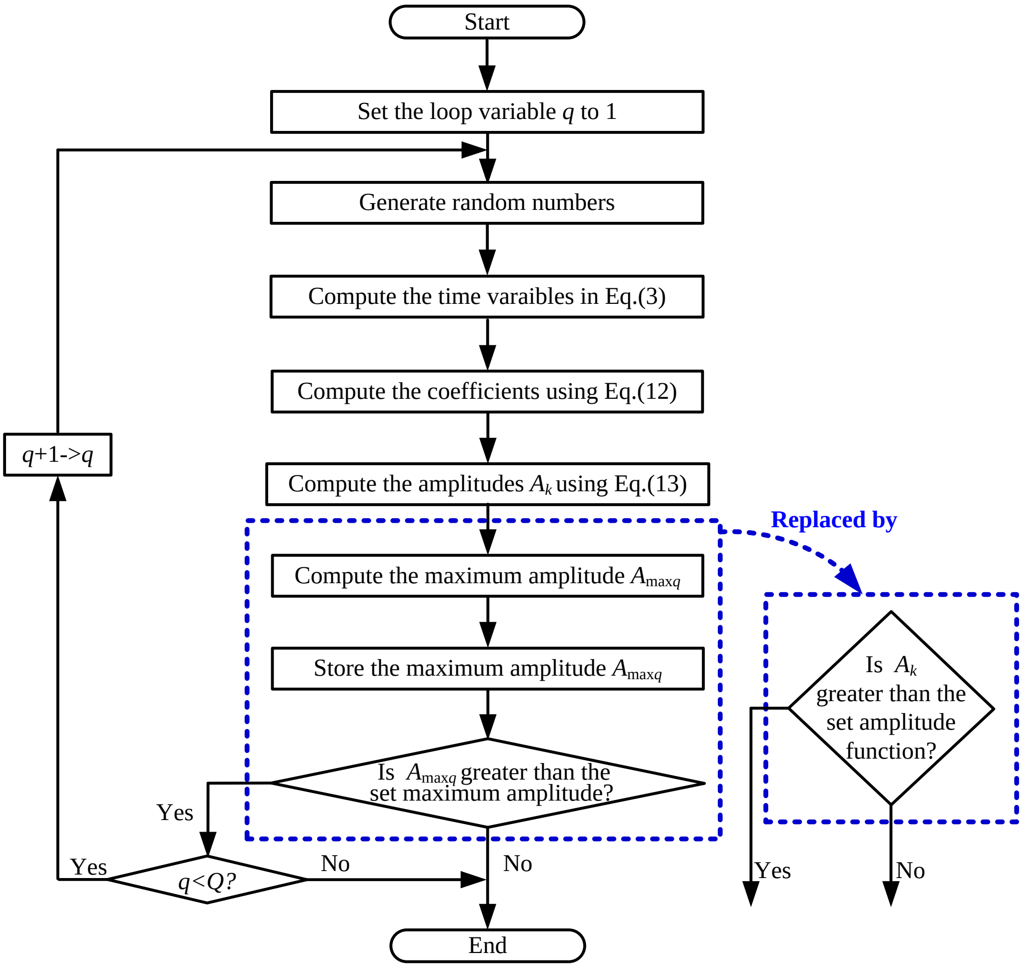

Figure 3. Harmonic Amplitude Customization and Optimization Algorithm for the SVPWM Strategy

Step 1: Set the customization and optimization parameters: the maximum iteration number Q, and the required maximum harmonic amplitude $A_{\max}$. Set the loop variable q to 0. The variable q controls the iteration number.

Step 2: Generate the random numbers for the random variables in Equations (2) and (3). The number of the random variables depends on the random strategy. For example, the random zero-vector distribution SVPWM (RZDPWM) scheme requires one random variable R_0, and the random pulse position SVPWM (RPPPWM) scheme requires 3 random variables R_1, R_2 and R_3. If the four variables R_0, R_1, R_2 and R_3 are randomized, a hybrid random SVPWM (HRPWM) scheme is gotten.

Step 3: Compute the duration time in Equation (3). First of all, the sextant order number where the reference/command $\vec{U}_s$ resides is determined. In addition, the duration time T_1, T_2 and T_0 is computed. Finally, t_i ($i = 1,2,3,4,5,6,7$) is computed using Equations (2) and (3) based on the generated random number in Step 2.

Step 4: Compute the coefficients using Equation (12). The leading edge t_b and the trailing edges t_e of the rectangular pulse shown in Figure 1 and Figure 2 are determined by t_i ($i = 1,2,3,4,5,6,7$) in Equation (3). Then $c_k (k = 1,2,3,\cdots)$ is computed using a loop procedure.

Step 5: Compute the amplitudes using Equation (13) using the harmonic coefficients given in Step 4.

Step 6: Compute the maximum amplitude $A_{\max q} = \max\{A_k\}\big|_{k=1,2,3,\cdots}$. The harmonic needs to be truncated in the actual computation.

Step 7: Store the maximum amplitude $A_{\max q}$ in an array.

Step 8: Judge the iterative termination or continuation. If $A_{\max q} > A_{\max}$ and $q < Q$, the iteration continues, $q+1 \to q$ and go to Step 2; or else, the iteration terminates.

The above algorithm customizes the harmonic amplitude-frequency characteristic through controlling the maximum harmonic amplitude in Step 6, 7 and 8. Through controlling all the harmonic amplitudes, another algorithm is gotten. As shown in Figure 3, through setting a maximum curve of the amplitude-frequency characteristic $A_{\max}(k)$, the computed amplitude A_k given by Equation (13) is compared with $A_{\max}(k)$. If $A_k \le A_{\max}(k)$, the random numbers generated in Step 2 satisfy the customization requirement. Or else, the new random numbers should be generated, and the iteration continues.

5. Examples and Results

5.1. Computation Example 1: Harmonic Spectrum for the Deterministic SVPWM

The DC bus voltage U_{DC} is 100V, the fundamental wave frequency is 60Hz, and the switching frequency is 2160Hz. The maximum harmonic amplitudes of the line AB voltage are computed using Equation (13) and shown in Figure 4, corresponding to the modulation index from 0.05 to 1.15 for the deterministic SVPWM strategy. That is to say, R_0, R_1, R_2 and R_3 are set as 0.5, which is always called the symmetrical 7-segment SVPWM strategy. The harmonic spectra of the line voltage AB are shown in Figure 5, and Figure 6, given that the modulation indexes M are 0.6 and 0.9, respectively. Figure 5, and Figure 6, show that the harmonics with the maximum amplitudes, for example 0.662 and 0.345 for the modulation indexes M are 0.6 and 0.9 respectively, appear around the double switching frequencies, for example 72nd harmonic here. This is because of that the pulses shown in Figure 1, are symmetrical in each switching period.

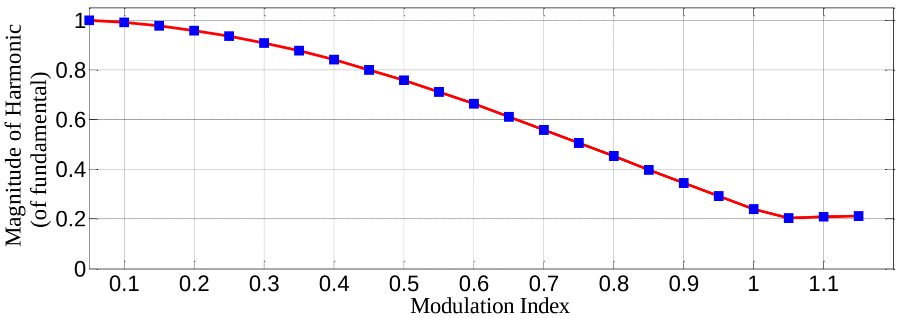

Figure. 4. Maximum Harmonic Amplitudes of the Line AB Voltage for the Deterministic SVPWM Strategy

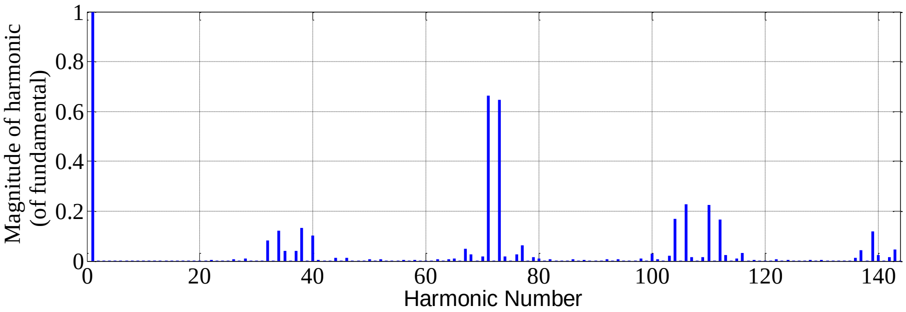

(a) Harmonic Spectra of the Line Voltage AB Plotted Using the Linear Scale

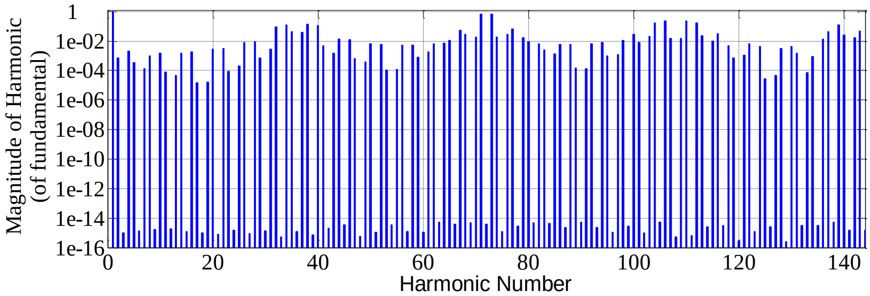

(b) Harmonic Spectra of the Line Voltage AB Plotted Using a Base 10 Logarithmic Scale for the Magnitude-axis and a Linear Scale for the Harmonic Number-axis

Figure 5. The Computation Results for the Symmetrical 7-Segment SVPWM Strategy and the Modulation Index 0.6

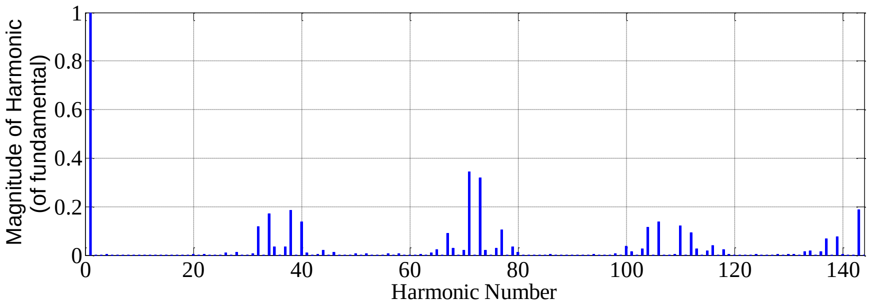

(a) Harmonic Spectra of the Line Voltage AB Plotted Using the Linear Scale

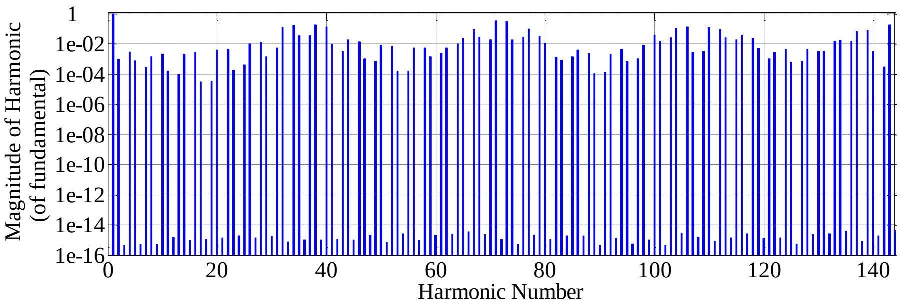

(b) Harmonic Spectra of the Line Voltage AB Plotted Using a Base 10 Logarithmic Scale for the Magnitude-axis and a Linear Scale for the Harmonic Number-axis

Figure 6. The Computation Results for the Symmetrical 7-Segment SVPWM Strategy and the Modulation Index 0.9

5.2. Computation Example 2: Random Zero-vector Distribution SVPWM

The test computation example described by Section 5.1 with the same previous parameters is used again but now with that the duration time ratio R_0 (in Equation (2)) of the two zero basic vectors is a random variable. In theory the random variable R_0 can be absolutely randomized with infinitely many real numbers which, however, actually is unnecessary or unpractical. The random variable is represented using the pseudorandom numbers which are always generated using the certain algorithm or the predefined array stored in the read-only memory in the practical application. The pseudorandom number generator can usually only generate a finite number of random numbers. So does the predefined array. The pseudorandom number therefore is periodical with the period R_p. There are S periods R_p in a fundamental period T_0. Given that the maximum iteration number Q =5000, the values of the random variable R_0 are drawn from the uniform distribution in the open interval (0,1), the computation results are shown in Figure 8, for the pseudorandom number periods are 3, 6 and 9 that are corresponding to $S=12$, $S=6$ and $S=4$, respectively. The maximum harmonic amplitudes and the corresponding random numbers for R_0 are given in Table 1, and Table 2, to an accuracy of four decimal places. Figure 9, and Figure 10, show the harmonic spectra for the modulation indexes M are 0.6 and 0.9 respectively.

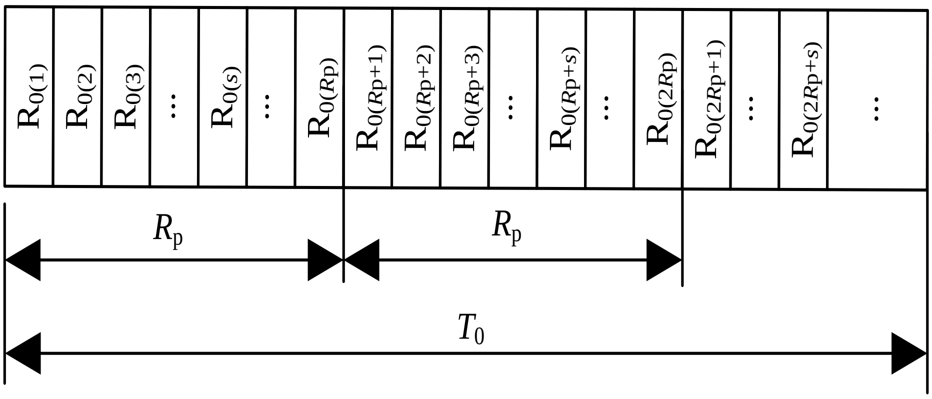

Figure 7. Relationship between the Fundamental Period and the Pseudorandom Number Period for the RZDPWM Scheme

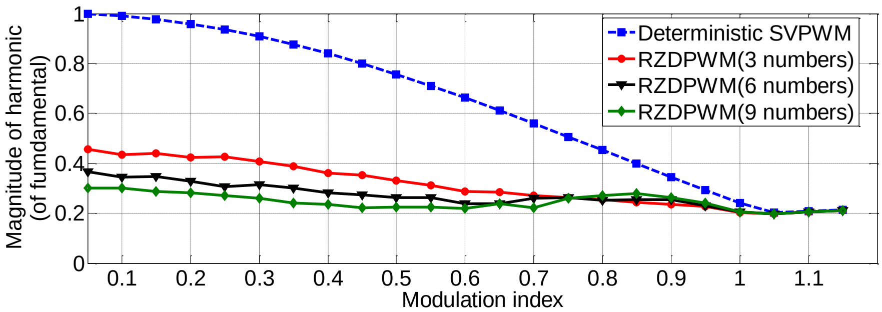

Figure 8. Maximum Harmonic Amplitudes of the Line AB Voltage for the RZDPWM Scheme with 5000 Iterations

Table 1. Maximum Amplitudes and the 3 Random Numbers for RZDPWM

Modulation index M	Maximum amplitude	3 random numbers for R_0		
0.05	0.4556	0.7900	0.3185	0.5341
0.10	0.4356	0.6290	0.8537	0.5014
0.15	0.4398	0.6132	0.8826	0.5250
0.20	0.4236	0.8729	0.4609	0.6533
0.25	0.4252	0.3253	0.8421	0.6170
0.30	0.4061	0.8830	0.4288	0.6963
0.35	0.3877	0.4359	0.7209	0.9071
0.40	0.3615	0.7479	0.8990	0.3838
0.45	0.3536	0.9238	0.3809	0.7643
0.50	0.3322	0.3070	0.0120	0.7856
0.55	0.3126	0.0365	0.7781	0.2352
0.60	0.2868	0.1808	0.0023	0.7634
0.65	0.2845	0.1262	0.7980	0.0048
0.70	0.2710	0.0161	0.0665	0.8221
0.75	0.2632	0.0139	0.0150	0.8263
0.80	0.2547	0.0187	0.9456	0.0294
0.85	0.2428	0.9482	0.9950	0.0028
0.90	0.2361	0.9911	0.0203	0.9960
0.95	0.2280	0.9606	0.9819	0.0232
1.00	0.2035	0.9733	0.9471	0.0187
1.05	0.1968	0.0199	0.0146	0.0240
1.10	0.2051	0.0042	0.0169	0.0281
1.15	0.2119	0.3840	0.0099	0.0134

From Figures 8, 9, and 10, it can be found that the RZDPWM scheme has excellent performance in suppressing the harmonic amplitude peak (or the maximum harmonic amplitude). The maximum harmonic amplitude is suppressed by more than 50 percent compared with the deterministic SVPWM strategy given that the pseudorandom number period is 4 and the modulation index is less than 0.7. The suppressing effect for the period 9 is more outstanding than the periods 6 and 3. The performance goes more and more excellent with the pseudorandom number period R_p becoming larger and larger on the whole, for example 3 to 9 in Figure 8, the reason of which is that more pseudorandom numbers means more degrees of freedom for searching the minimum harmonic amplitude peak. The proposed customization algorithm can be defined as a constrained optimization problem expressed as Equation (14).

Table 2. Maximum Amplitudes and the 6 Random Numbers for RZDPWM

Modulation index M	Maximum amplitude	6 random numbers for R_0					
0.05	0.3675	0.8421	0.7030	0.6584	0.8747	0.4738	0.0799
0.10	0.3436	0.3428	0.1707	0.1899	0.8808	0.0670	0.5779
0.15	0.3482	0.6910	0.4789	0.3010	0.8754	0.5706	0.8880
0.20	0.3283	0.5169	0.8232	0.5473	0.2632	0.0947	0.7807
0.25	0.3075	0.8660	0.5769	0.2408	0.4430	0.1705	0.1514
0.30	0.3138	0.8586	0.9413	0.2394	0.7529	0.3733	0.5461
0.35	0.3017	0.9370	0.3963	0.5480	0.1460	0.3425	0.0215
0.40	0.2826	0.8598	0.0601	0.1065	0.4329	0.1726	0.6114
0.45	0.2732	0.6393	0.8979	0.9983	0.1190	0.7889	0.3567
0.50	0.2642	0.4758	0.9550	0.8731	0.5198	0.0442	0.9011
0.55	0.2631	0.8340	0.3571	0.7465	0.0432	0.0230	0.0328

0.60	0.2387	0.0124	0.9172	0.3471	0.6942	0.9768	0.9221
0.65	0.2378	0.9310	0.8719	0.0137	0.9380	0.0498	0.8364
0.70	0.2607	0.9067	0.9804	0.9278	0.9959	0.0141	0.4241
0.75	0.2621	0.9951	0.0391	0.1958	0.9011	0.1082	0.9777
0.80	0.2512	0.9019	0.9975	0.9542	0.0566	0.9400	0.0097
0.85	0.2551	0.9603	0.9834	0.9264	0.0261	0.0638	0.9374
0.90	0.2534	0.9984	0.0970	0.9723	0.7401	0.8486	0.9846
0.95	0.2298	0.9992	0.9776	0.5559	0.9810	0.0108	0.9540
1.00	0.2048	0.9902	0.9785	0.5124	0.1301	0.0064	0.9665
1.05	0.1980	0.0516	0.0516	0.2872	0.0406	0.0030	0.0517
1.10	0.2054	0.4065	0.0979	0.0011	0.0841	0.1097	0.0228
1.15	0.2119	0.9256	0.0059	0.0529	0.6870	0.0640	0.0130

$$\begin{cases} \min \quad \max\left\{2\left|\dfrac{\mathrm{j}}{kT_0\omega_0}\sum_{i=1}^{N}\left(\mathrm{e}^{-\mathrm{j}k\omega_0 t_{ei}} - \mathrm{e}^{-\mathrm{j}k\omega_0 t_{bi}}\right)\right|\right\}\Bigg|_{R_1=\frac{1}{2},R_2=\frac{1}{2},R_3=\frac{1}{2}} \\ \text{s.t.} \quad 0 \le R_{0(s)} = R_{0(R_\mathrm{p}+s)} = R_{0(2R_\mathrm{p}+s)} = \cdots = R_{0((S-1)R_\mathrm{p}+s)} \le 1 \qquad (s=1,2,3\cdots,R_\mathrm{p}-1) \end{cases} \tag{14}$$

There are R_p independently optimization variables in Equation (14). The most excellent case is that the number of the independently optimization variables is equal to the number of the switching periods in a fundamental period, for example 2160Hz/60Hz=36 in this example. It should be pointed out that the maximum harmonic amplitude suppressing effect increases insignificant if the pseudorandom period R_p increases to a certain value. The RZDPWM scheme has advantageous maximum harmonic amplitude suppressing effect for the small modulation index from Figure 8, because the total duration time T_0 (that is $T_{00}+T_{07}$) for the zero vectors $\vec{U}_0$ and $\vec{U}_7$ is long enough for randomization to suppress the harmonic amplitude peak.

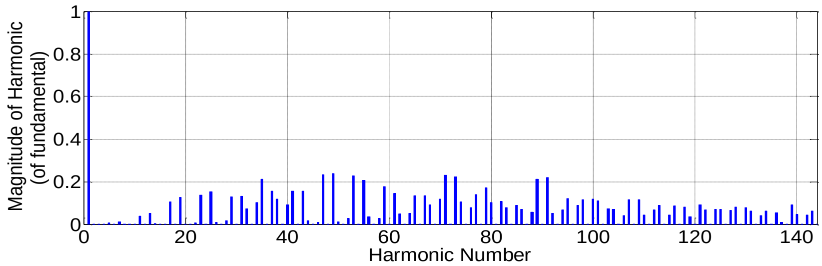

(a) Harmonic Spectra of the Line Voltage AB Plotted Using the Linear Scale

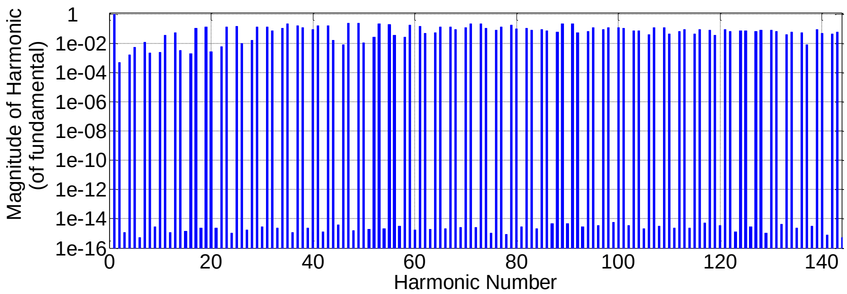

(b) Harmonic Spectra of the Line Voltage AB Plotted Using a Base 10 Logarithmic Scale for the Magnitude-axis and a Linear Scale for the Harmonic Number-axis

Figure 9. The Optimization Results for the RZDPWM Scheme with 6 Random Numbers (0.0124, 0.9172, 0.3471, 0.6942, 0.9768, 0.9221) and the Modulation Index 0.6

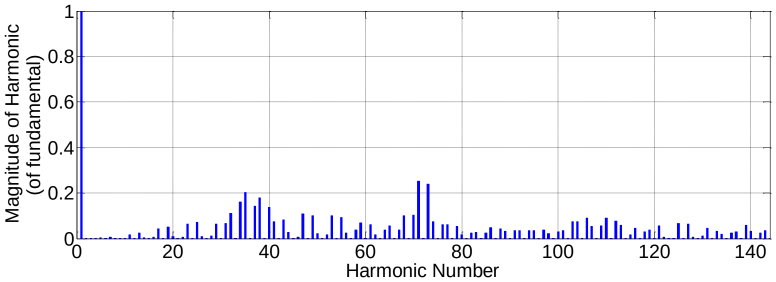

(a) Harmonic Spectra of the Line Voltage AB Plotted Using the Linear Scale

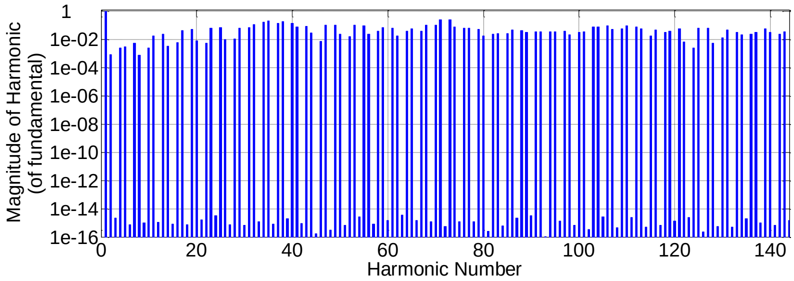

(b) Harmonic Spectra of the Line Voltage AB Plotted Using a Base 10 Logarithmic Scale for the Magnitude-axis and a Linear Scale for the Harmonic Number-axis

Figure 10. The Optimization Results for the RZDPWM Scheme with 6 Random Numbers (0.9984, 0.0970, 0.9723, 0.7401, 0.8486, 0.9846) and the Modulation Index 0.9

5.3. Computation Example 3: Random Pulse Position SVPWM

The test computation example described by Section 5.2 with the same previous parameters is used again but now with that the three variables R_1, R_2 and R_3 (that control the three-phase pulse position in Equation (2)) are set as random variables. The values of the three random variables are drawn from the uniform distribution in the open interval (0,1), the computation results are shown in Figure 11, for the pseudorandom number periods are 3, 6 and 9 respectively. The maximum harmonic amplitude is 0.2119 and the corresponding random numbers ([R_1],[R_2],[R_3]) are ([0.0663, 0.9081, 0.2587, 0.2357, 0.9942, 0.9117], [0.6007, 0.2791, 0.1201, 0.9638, 0.2492, 0.5071], [0.2986, 0.0741, 0.3158, 0.6488, 0.7784, 0.0880]) for the modulation index 0.6, and the harmonic spectrum is shown in Figure 12. The maximum harmonic amplitude is 0.2119 and the corresponding random numbers ([R_1], [R_2],[R_3]) are ([0.3844, 0.9123, 0.1749, 0.8407, 0.9176, 0.0238], [0.1863, 0.6193, 0.0428, 0.7177, 0.9029, 0.7287], [0.5901, 0.2796, 0.3435, 0.6943, 0.0775, 0.9492]) for the modulation index 0.9, and the harmonic spectrum is shown in Figure 13.

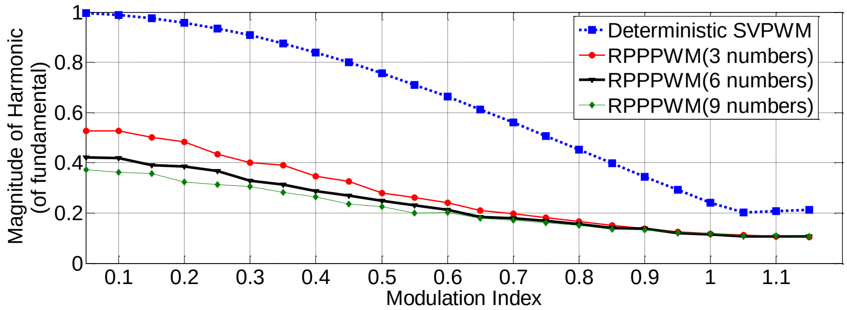

Figure 11. Maximum Harmonic Amplitudes of the Line AB Voltage for the RPPPWM Scheme with 5000 Iterations

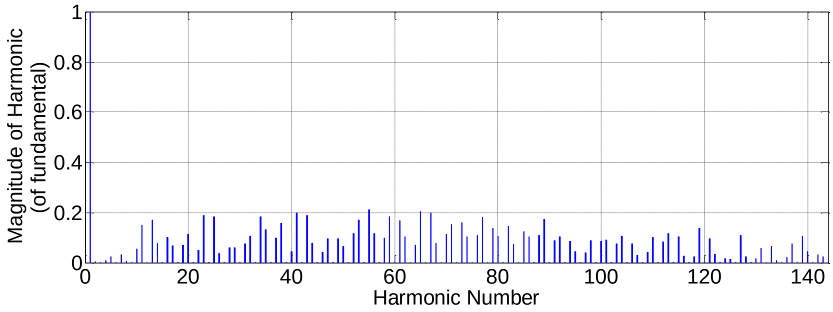

(a) Harmonic Spectra of the Line Voltage AB Plotted Using the Linear Scale

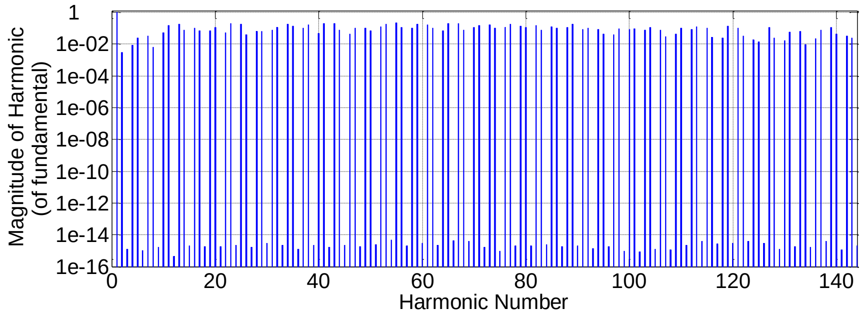

(b) Harmonic Spectra of the Line Voltage AB Plotted Using a Base 10 Logarithmic Scale for the Magnitude-axis and a Linear Scale for the Harmonic Number-axis

Figure 12. The Optimization Results for the RPPPWM Scheme with 6 Random Numbers and the Modulation Index 0.6

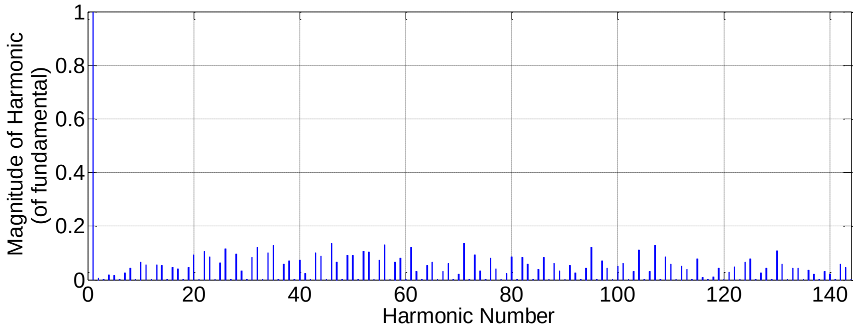

(a) Harmonic Spectra of the Line Voltage AB Plotted Using the Linear Scale

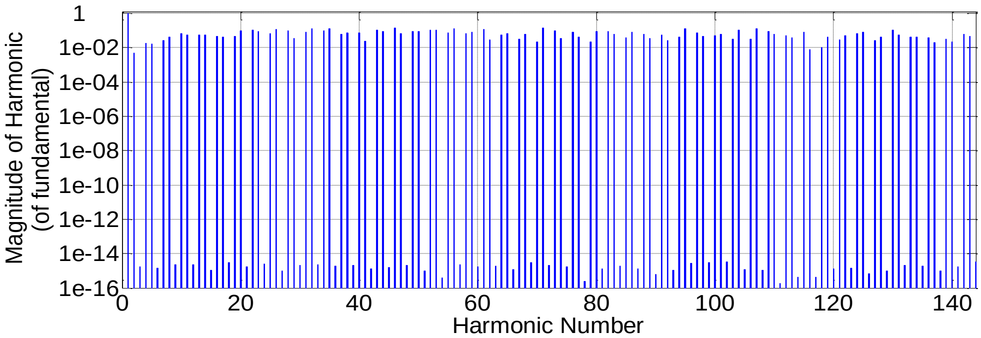

(b) Harmonic Spectra of the Line Voltage AB Plotted Using a Base 10 Logarithmic Scale for the Magnitude-axis and a Linear Scale for the Harmonic Number-axis

Figure 13. The Optimization Results for the RPPPWM Scheme with 6 Random Numbers and the Modulation Index 0.9

5.4. Computation Example 3: Hybrid Random SVPWM

The test computation example described by Section 5.2 with the same previous parameters is used again but now with that the four variables R_0, R_1, R_2 and R_3 (in Equations (2) and (3)) are set as random variables. The values of the four random variables are drawn from the uniform distribution in the open interval (0,1), the computation results are shown in Figure 14, for the pseudorandom number periods are 3, 6 and 9 respectively. The maximum harmonic amplitude is 0.2119 and the corresponding random numbers ([R_0], [R_1],[R_2],[R_3]) are ([0.4687, 0.4645, 0.1601, 0.8044, 0.7551, 0.2509], [0.0331, 0.8106, 0.4949, 0.4908, 0.8258, 0.5000], [0.2506, 0.6706, 0.6850, 0.3265, 0.3559, 0.2176], [0.9724, 0.1274, 0.7654, 0.1125, 0.5090, 0.0450]) for the modulation index 0.6, and the harmonic spectrum is shown in Figure 15. The maximum harmonic amplitude is 0.2119 and the corresponding random numbers ([R_0], [R_1],[R_2],[R_3]) are ([0.7422, 0.2701, 0.9815, 0.1340, 0.3200, 0.2784], [0.9393, 0.7642, 0.8166, 0.7795, 0.3424, 0.1445], [0.5973, 0.7775, 0.4597, 0.0691, 0.8175, 0.2905], [0.1799, 0.3396, 0.5625, 0.5375, 0.2763, 0.3257],) for the modulation index 0.9, and the harmonic spectrum is shown in Figure 16.

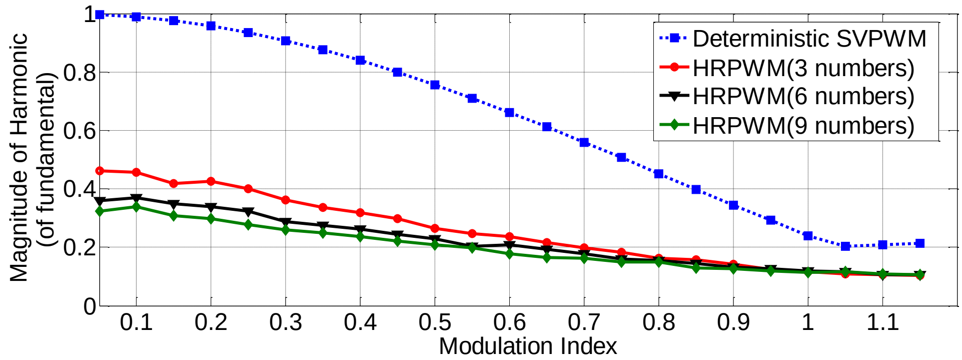

Figure 14. Maximum Harmonic Amplitudes of the Line AB Voltage for the HRPWM Scheme with 5000 Iterations

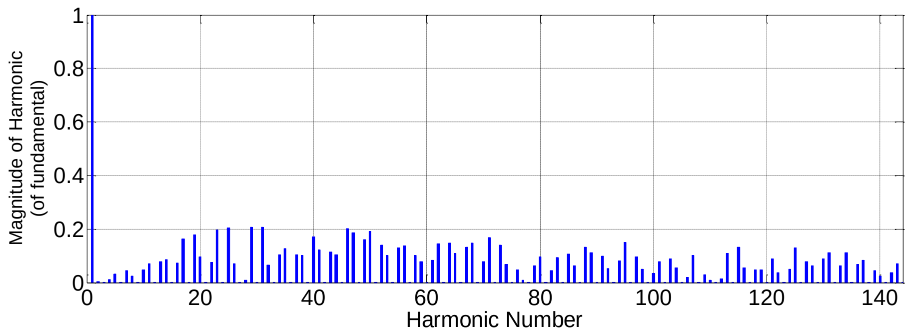

(a) Harmonic Spectra of the Line Voltage AB Plotted Using the Linear Scale

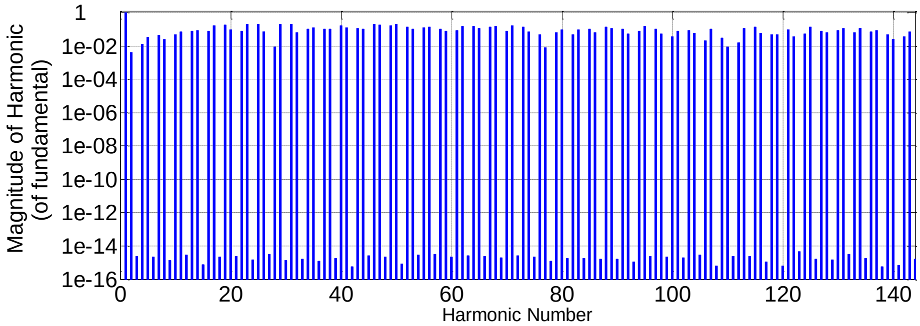

(b) Harmonic Spectra of the Line Voltage AB Plotted Using a Base 10 Logarithmic Scale for the Magnitude-axis and a Linear Scale for the Harmonic Number-axis

Figure 15. The Optimization Results for the HRPWM Scheme with 6 Random Numbers and the Modulation Index 0.6

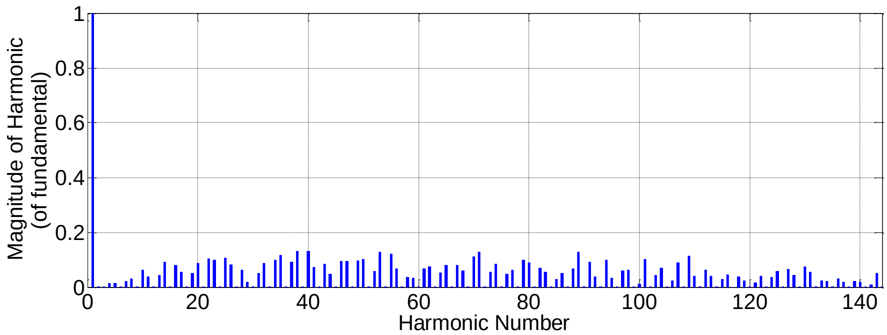

(a) Harmonic Spectra of the Line Voltage AB Plotted Using the Linear Scale

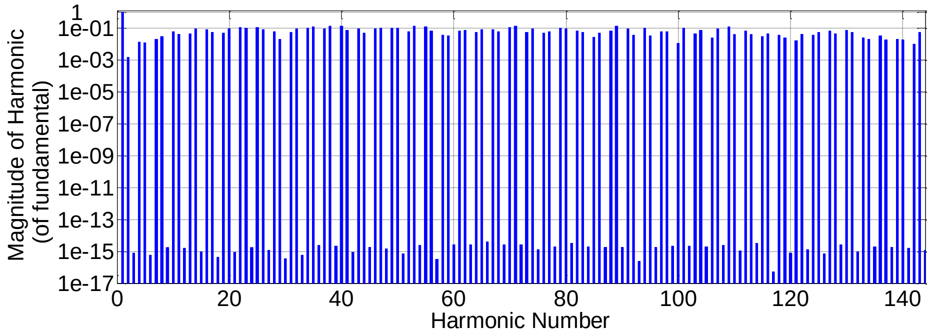

(b) Harmonic Spectra of the Line Voltage AB Plotted Using a Base 10 Logarithmic Scale for the Magnitude-axis and a Linear Scale for the Harmonic Number-axis

Figure 16. The Optimization Results for the HRPWM Scheme with 6 Random Numbers and the Modulation Index 0.9

5.5. Comparison of Several Different Modulation Strategies

The maximum harmonic amplitudes in comparison mode for the deterministic SVPWM strategy and three schemes of the random SVPWM strategy are shown in Figure 17. In order to be intuitively compared, the maximum harmonic amplitudes are revealed in three different aspects: the absolute amplitudes in Figure 17(a), the relative amplitudes in Figure 17(b), and the decrease amount of the amplitude in Figure 17(c). It should be noticed that the computation accuracy based on the Monte Carlo method highly depends on the maximum iteration number. The identical results cannot be gotten for the random strategy during the two runs of the proposed algorithm because of the randomization.

Based on the computation results from 5000 iterations for the Monte Carlo method, some valuable findings can be made. The random SVPWM strategy has outstanding effects on suppressing the maximum harmonic amplitude/magnitude and spreading the harmonic spectrum to a wide range. The maximum harmonic amplitude is reduced by more than 40% compared with the deterministic strategy. The RPPPWM scheme has the most excellent performance because it makes full use of the degrees of freedom of the zero vector distribution and the pulse positioning. However, it seems that (a) the RZDPWM has more excellent performance than RPPPWM for that the modulation index is smaller than 0.5 from Figure 17, and (b), there is no notable difference between the RPPPWM and HRPWM schemes. There are 4 optimization variables for the RPPPWM scheme while only one optimization variable for the RZDPWM scheme and 3 optimization variables for the RPPPWM scheme, which makes it more difficult in finding the maximum value for the RPPPWM objective function. If a large iteration number is adopted, the maximum harmonic amplitudes of the HRPWM scheme should be smaller than the RZDPWM and RPPPWM schemes. The RZDPWM scheme has excellent performance for the small modulation index, while RPPPWM scheme has the opposite characteristic. The HRPWM scheme has excellent performance over the entire linear modulation range with the modulation index from 0 to $2/\sqrt{3}$. The performance of the RZDPWM scheme grows worse and worse with the modulation index becoming larger and larger because the duration time for the zero vector, meanwhile, becomes shorter and shorter. The obvious modulation index threshold is 0.55 that can be found in Figure 17. This threshold value is most likely 0.577, half of the maximum linear modulation index $2/\sqrt{3}$, which needs further study. If the customization function for the maximum amplitude is shown in Figure 17(a), the customization procedure can be accomplished within 5000 iterations based on the proposed algorithm.

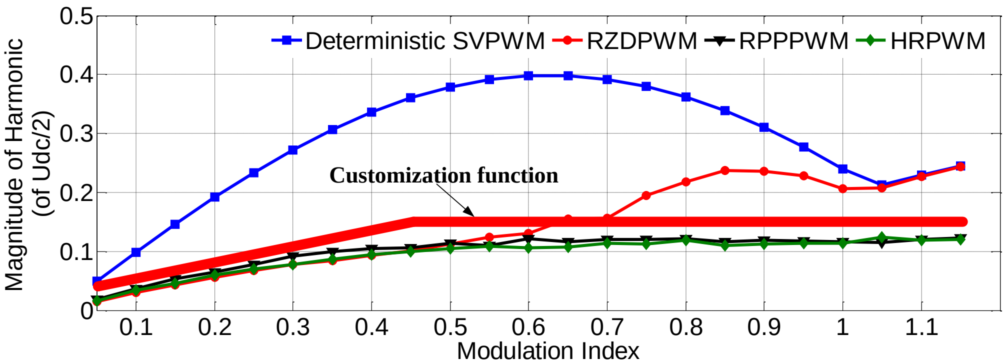

(a) Absolute Amplitude to Udc/2

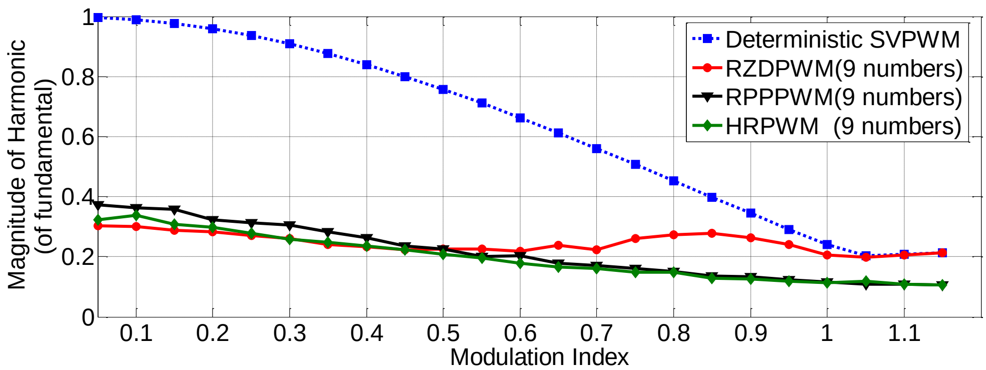

(b) Relative Amplitude to the Fundamental

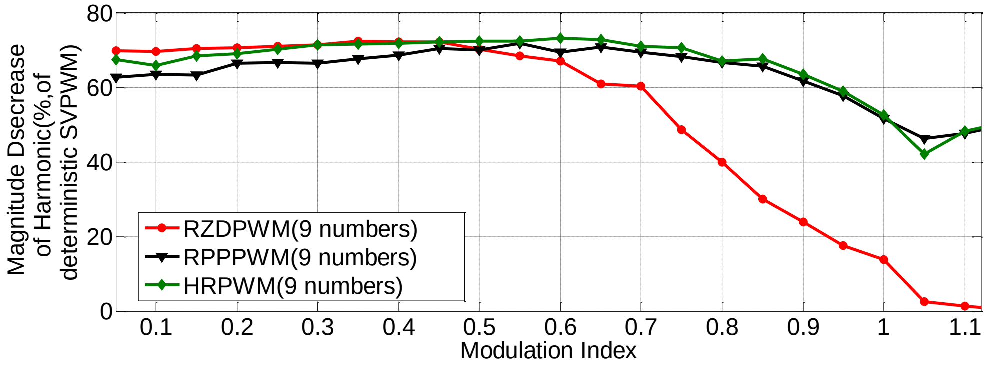

(c) Amplitude Decrease to the Fundamental of the Deterministic Strategy

Figure 17. Maximum Harmonic Amplitudes of the Line AB Voltage for Several Different Strategies with 5000 Iterations

6. Conclusions

A harmonic optimization and customization algorithm is proposed for the random SVPWM strategy. The theoretical spectrum computation method is given for the SVPWM strategy and the corresponding formulas are presented firstly. In addition, the key procedure of the proposed algorithm is presented. Finally, several computation examples are provided to verify the effectiveness and feasibility. The results and analysis show that the proposed algorithm has several advantages. Firstly, the algorithm is based on the assumption that the random variable (in the random strategy) is implemented by the periodical pseudorandom number, so it has sufficient convenience to analyze the harmonic spectrum using the Fourier series for the periodical function. The assumption is consistent with the practical application. In addition, the optimization and customization algorithm is realized using the Monte Carlo method. This is highly convenient and feasible because the objective function is extremely complicated and the traditional optimization method does not work efficiently for this case. The random sampling characteristic of the Monte Carlo method is efficiently made full use of to find the maximum harmonic amplitude. Finally, the proposed algorithm is proved efficient through test examples. In theory, the extremely high accuracy can be gotten through a large enough iteration number and using the engineering computation software package. For example, the powerful functions and high precision features of MATLAB can be made full use of. However, it should be noticed that the harmonic characteristic is extremely complicated and this study only analyzes the case for some fundamental frequency and switching frequency. Our future study is to work on the universal law that can assess the maximum harmonic amplitude to an arbitrary frequency.

Acknowledgments

This work is supported by National Science Foundation of China (No. U1304525). This paper is a revised and expanded version of a paper entitled, “Harmonic Frequency Spectrum Customization Method to Random Space Vector Pulse Width Modulation”, presented at the 5th International Conference on Information Science and Industrial Applications (ISI 2016) in Harbin, China on August 19-20, 2016. The authors would like to thank the anonymous reviewers for their valuable work.

References

[1] M. Xiaolin, J. A. Kumar and A. Rajapandian, “Hybrid interleaved space vector PWM for ripple reduction in modular converters”, IEEE Transactions on Power Electronics, vol. 26, no. 7, **(2011)**, pp. 1954-1967.

[2] D. G. Holmes and T. A. Lipo, "Pulse width modulation for power converters: principles and practice", IEEE Press, USA, **(2003)**.
[3] B. A. Rahiman, K. Saikrishna, A. H. Khalifa and D. Apparao, "Space-vector-based synchronized three-level discontinuous PWM for medium-voltage high-power VSI", IEEE Transactions on Industrial Electronics, vol. 61, no. 8, **(2014)**, pp. 3891-3901.
[4] K. Shahriyar, M. Javad and A. Ali, "Application of random PWM technique for reducing the conducted electromagnetic emissions in active filters", IEEE Transactions on Industrial Electronics, vol. 54, no. 4, **(2007)**, pp. 2333~2343.
[5] S. H. Na, Y. G. Jung, Y. C. Lim and S. H. Yang, "Reduction of audible switching noise in induction motor drives using random position space vector PWM", IEE Proceedings Electric Power Applications, vol. 149, no. 3, **(2002)**, pp. 195~200.
[6] D. Jiang and F. (Fred) Wang, "Variable switching frequency PWM for three-phase converters based on current ripple prediction", IEEE Transactions on Power Electronics, vol. 28, no. 11, **(2013)**, pp. 4951-4961.
[7] G. Chen, Z. Wu and Y. Zhu, "Harmonic analysis of random pulse position space vector PWM", Journal of Tongji University, vol. 40, no. 7, **(2012)**, pp. 1111-1117.
[8] Z. Wu, G. Chen, Y. Zhu and G. Tian, "Harmonic analysis of random zero-vector distribution space vector pulse-width modulation", Journal of Tongji University, vol. 39, no. 9, **(2011)**, pp. 901-907.
[9] G. Chen, M. Zhang and J. Zhao, "Harmonic distortion factor of A hybrid space vector PWM based on random zero-vector distribution and random pulse position", Advances in Information Sciences and Service Sciences, vol. 4, no. 16, **(2012)**, pp. 242-250.
[10] S. Albatran, Y. Fu Yong and A. Albanna, "Comprehensive mathematical description and harmonic analysis of hybrid two-dimensional-three-dimensional space vector modulation", IEEE Transactions on Industrial Electronics, vol. 61, no. 7, **(2014)**, pp. 3327-3336.
[11] J. Holtz, M. Holtgen and J. O. Krah, "A space vector modulator for the high-switching frequency control of three-level SiC inverters", IEEE Transactions on Power Electronics, vol. 29, no. 5, **(2014)**, pp. 2618-2626.
[12] G. Chen and J. Kang, "Harmonic analysis of a random zero vector distribution space vector pulse width modulation", International Journal of Signal Processing, Image Processing and Pattern Recognition, vol. 9, no. 6, **(2016)**, pp. 227-240.
[13] G. Chen and J. Kang, "Harmonic frequency spectrum customization method to random space vector pulse width modulation", Advanced Science and Technology Letters, vol. 138, **(2016)**, pp. 215-219.

Author

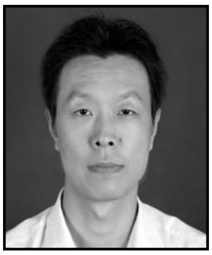

Guoqiang Chen, he is currently an associate professor in the School of Mechanical and Power Engineering, Henan Polytechnic University, China. His research interests include robot technology, electric vehicle control, motor control and pulse width modulation technology.